Available online at www.sciencedirect.com
SCIENCE DIRECT®
European Journal of Medicinal Chemistry 38 (2003) 413–419
EUROPEAN JOURNAL OF MEDICINAL CHEMISTRY
www.elsevier.com/locate/ejmech

Homology modelling and docking studies on Varicella Zoster Virus Thymidine kinase

Loredana Spadola [a,b], Ettore Novellino [a], Gerd Folkers [b], Leonardo Scapozza [b,*]

[a] *Dipartimento di Chimica Farmaceutica e Tossicologica, Università di Napoli, Via D. Montesano 49, 80131 Napoli, Italy*
[b] *Department of Applied Biosciences, Institute of Pharmaceutical Sciences, ETH Zürich, Winterthurerstr. 190, 8057 Zurich, Switzerland*

Received 10 October 2002; accepted 14 December 2002

Abstract

Thymidine kinase (TK) is the key enzyme in antiviral and suicide gene therapies. While herpes simplex virus type 1 thymidine kinase has been widely studied and crystallised less is known on Varicella Zoster Virus thymidine kinase (VZV TK) and its three-dimensional structure. In this paper we report the model of the three-dimensional structure of VZV TK resulting from a homology modelling study. Subsequent docking studies of the natural substrate deoxythymidine (dT) and known antiviral drugs were performed and shaded new light on the binding characteristics of the enzyme.

Keywords: Antiviral therapy; Varicella Zoster; Homology modelling; Molecular docking

1. Introduction

Varicella Zoster Virus (VZV) is a member of the herpesvirus family, which includes widely spread, enveloped, double-stranded DNA viruses. VZV belongs to the alphaherpesvirus group, and is related most closely to herpes simplex virus type 1 and 2, based upon DNA sequence similarities and the linear organisation of the viral genome [1–4]. The virus causes varicella (chicken pox) and herpes zoster (shingles). The course of varicella is generally benign, but in immunocompromised patients, transplant recipients (e.g. Bone Marrow Transplantation) and cancer patients, VZV infections can be life-threatening [5–7]. In recent years, progresses made in understanding the biochemical mechanisms involved in intracellular replication of viruses allowed the development of antiviral agents, which interfere with the virus specific functions or interact with virus specific enzymes. The specificity of many of these drugs is mainly due to the selective in vivo activation by the viral thymidine kinase (TK). TK catalyses the phosphorylation of thymidine (dT) to thymidine monophosphate (dTMP) in the presence of ATP and Mg^{2+}. The most relevant difference between viral and human TK on which therapeutic interventions, such as antiviral and suicide gene therapy [8,9], are based, relies on the substrate acceptance: while human TK only accepts its natural substrate (dT), viral TKs can bind a broad spectrum of purine and pyrimidine derivatives including those with acyclic sugar moieties [10–17].

Varicella Zoster Virus thymidine kinase (VZV TK) has been recently isolated as recombinant highly purified enzyme and crystals were obtained [18]. However, despite these experimental progresses, no structural information is available yet. Knowledge on the structure of the active site of TK, as well as the interactions of the binding site amino acids with the substrate, would facilitate the development of new drugs. For this reason, the three-dimensional model of VZV TK was built using homology modelling based on herpes simplex virus type 1 thymidine kinase (HSV-1 TK) structure as template [19–23]. The stability of the model was assessed with molecular dynamics simulations and the model itself was used for docking studies aimed at understanding binding characteristics of the enzyme at molecular level.

* Corresponding author.
E-mail address: leonardo.scapozza@pharma.anbi.ethz.ch (L. Scapozza).

0223-5234/03/$ - see front matter
doi:10.1016/S0223-5234(03)00053-9

2. Methods

2.1. Homology modelling

Homology modelling studies on VZV TK were carried out based on the alignment with the sequence of HSV-1 TK (Fig. 1) and on its structure [19]. The sequence alignment was performed by using the GeneStream Resource Server [24]: the identity percentage is 29.9% while the homology is 64.8%. The model was built, starting from the methionine indicated with the number 2 in Fig. 1, by mutating the amino acids of the template with the program SYBYL 6.8 [25] in accordance to the protein sequence of VZV TK and its alignment with HSV-1 TK. Missing loops have been modelled using the loop search routine of SYBYL 6.8. The resulting model was submitted to energy minimisation and molecular dynamics simulations in explicit water. Regions of 'deletions' and 'insertions', corresponding to amino acids (highlighted in bold in Fig. 1) 2–6; 21–38; 102–113; 207–227; 236–247; 311–331, have been treated using a two-step protocol including energy minimisation followed by simulated annealing (SA). Before starting the minimisation the quality of the geometry of our model was checked using the program PROCHECK [26]. The quality of the overall structure was comparable with that of the template structure as determined by X-ray. The energy minimisation was carried out using the program AMBER 5.0 [27], according to the following protocol: all hydrogen atoms were added to the protein that was then immersed in a cube of 7.5 Å of Monte Carlo waters. The complete interaction was calculated and a constant dielectric function was used for the electrostatic energy. The primary cut-off distance for non-bonded interactions was set at 10 Å while the secondary cut-off, in order to take into account also long-range interactions, was set at 12 Å. Minimisation, using 1000 steps of steepest descent followed by conjugate gradient method, was carried out until the root-mean square deviation (rmsd) of the Cartesian elements of the gradient reached a value smaller than 0.15 Å. After the minimisation the bulk

```
                46  50        60        70           80        90
HSV QQEATEVRPEQKMPTLLRVYIDGPHGMGKTTTTQLLV---ALGSRDDIVYVPEPMTYWRV
    .  .:. . . ::  .:::.:.:: .:.:::::... ..   :. . . :. . ::.:::
VZV M--STD-KTDVKMG-VLRIYLDGAYGIGKTTAAEEFLHHFAI-TPNRILLIGEPLSYWRN
                2       10        20        30          40

          100       110       120       130       140
HSV LGASETIANIYTTQHRLDQGEISAGDAAVVMTSAQITMGMPYAVTDAVLAPHIGGEAGS-
    :.. ..: .:: :: :  .:..:  ::  . .  :  .  :.:.  : ..  .   ...
VZV LAGEDAICGIYGTQTRRLNGDVSPEDAQRLTAHFQSLFCSPHAIMHAKISALMDTSTSDL
     50        60        70        80        90       100

   150       160       170       180       190       200
HSV -SHAPPPALTLIFDRHPIAALLCYPAARYLMGSMTPQAVLAFVALIPPTLPGTNIVLGAL
     .    :   .. :::::::. .:.: .:::.:.:.: :. ...  .:   ::::.:. ..
VZV VQVNKEPYKIMLSDRHPIASTICFPLSRYLVGDMSPAALPGLLFTLPAEPPGTNLVVCTV
    110       120       130       140       150       160

   210       220       230       240       250       260
HSV PEDRHIDRLAKRQRPGERLDLAMLAAIRRVYGLLANTVRYLQCGGSWREDWGQLS-GTAV
       :.:.:.:: :::: ..: .. ..: :: .: ::. .:. . .:.  :. ::  . :
VZV SLPSHLSRVSKRARPGETVNLPFVMVLRNVYIMLINTIIFLKTN-NWHAGWNTLSFCNDV
    170       180       190       200       210       220

    270       280          290       300       310       320
HSV PPQGAEPQSNAGPR--PHIGDTLFTLFRAPELLAPNGDLYNVFAWALDVLAKRLRSMHVF
      :  . .     :  : : :::.... ::: .  :..  ..::...:..  ::: :
VZV FKQKLQKSECIKLREVPGIEDTLFAVLKLPELCGEFGNILPLWAWGMETLSNCSRSMSPF
     230       240       250       260       270       280

      330       340       350       360       370
HSV ILDYDQSPAGCRDALLQLTSGMVQTHVTTPGSIPTICDLARTFAREMGEAN
    .:. .:.:    . :  :   :. ..... :.   . .:. .    . ...
VZV VLSLEQTPQHAAQELKTLLPQMTPANMSS-GAWNILKELVNAV---QDNTS
     290       300       310       320          330
```

Fig. 1. Alignment of the sequences of HSV-1 and VZV TKs obtained with the GeneStream Resources Server [24]. The points between the sequences represent the degree of similarity between amino acids: 2 points, identical; 1 point, similar. In bold are shown the segments analysed separately with simulated annealing studies.

water was removed while water molecules within the binding site were kept and SA studies on the mentioned deletions and insertions regions were carried out. Five steps of SA, each one of 30 ps, were performed. The system in implicit water was heated starting from 50 to 450 K in 5 ps, and then we left it at 450 K for 20 ps and finally cooled to the initial temperature in 5 ps. Distance dependent dielectric constant was used. The time constant for heat bath coupling was set to different values in the different stages of the run: from 0 to 25 ps the constant was 0.2 in order to have a tight coupling for heating and equilibration, then we increased its value setting a slow cooling phase (25–27 ps), a faster cooling (27–29 ps) and a very fast cooling in the final part (29–30 ps). These variations allow smaller fluctuations in kinetic energy for the first part (0–25 ps) and a bigger freedom to the system in the final cooling part (25–30 ps). After the fifth step of SA we minimised the structure (all residues) with ADP and TMP according to the same procedure above described. Subsequently the resulting minimised structure was submitted to molecular dynamic simulations (MD) following this protocol: the system was solvated as described before; MD calculations were begun starting with initial velocities set to 0; the simulation was run for a total of 150 ps after equilibration with a time step of 2 fs and the SHAKE [28] algorithm was used in order to constrain bonds involving hydrogens. Harmonic restraints were imposed to ADP only. After the MD we calculated, with the CARNAL module of AMBER, the mean structure over the time length of the simulation and minimised it. This minimised structure, whose quality was evaluated with PROCHECK, was taken as final model.

2.2. Docking

Docking studies were carried out by using the program AUTODOCK 3.0 [29]. The protein and the ligands were prepared by using the program SYBYL 6.8 [25]. For protein only polar hydrogen atoms were kept and the charges were assigned according to the Kollman united-atom method. According to the results of Pospisil et al. [30] the water molecules within the thymidine binding site were removed only for the docking of guanine analogues. Atomic solvation parameters were assigned to the protein atoms using the ADDSOL utility. The grid maps around the protein binding site were calculated using AUTOGRID 3.0 with $61 \times 61 \times 61$ points, and a grid spacing of 0.375 Å.

For the ligands all hydrogens were added and Gasteiger–Huckel charges [31] were calculated. The utility AutoTors was used to define the rotatable bonds in the ligands.

We calculated 20 docking orientations for each ligand, and clustered them using a cluster tolerance to the root-mean-square positional deviation of 1.0 Å. The lowest energy orientations of each cluster were analysed.

3. Results and discussion

The structure of the VZV TK has not yet been elucidated although the enzyme has been recently obtained in its highly purified recombinant form [18]. In order to understand at a molecular level the binding characteristics of the enzyme we first carried out homology modelling studies based on the X-ray structure of HSV-1 TK [19–23]. The superimposition of our final model and the template shows that the typical αβ-fold of TK, with the core formed by a central five-stranded parallel β-sheet surrounded by 12 helices [19–23], is conserved. A more detailed analysis involves the substrate binding site. Fig. 2 shows the binding sites of VZV TK (Fig. 2a) and HSV-1 TK (Fig. 2b) with the substrate dTMP and reveals more details on substrate binding. A strong similarity between the two active sites is apparent, since most of the residues of VZV TK are conserved or substituted conservatively. In particular, the Watson–Crick hydrogen bonds with Gln82, in analogy to the one of HSV-1 TK formed by Gln125, are present, as well as the hydrogen bond between the 3′-OH group in the sugar moiety and the residues Tyr58 and Glu184. A hydrophobic sandwich-like interaction of the base-moiety with the residues Phe131 and Phe85 is characteristic of VZV TK, while the sandwich-like complex in HSV-1 TK is formed with residues Tyr172 and Met128 (Fig. 2). In contrary to the perfect alignment of Tyr172–base–Met128 in HSV-1 TK, the phenylalanine residues and the thymine ring in VZV TK are not perfectly aligned. The distance between each phenylalanine ring and the thymine moiety is around 3.6 Å. In addition, while a strong electrostatic interaction is present in HSV-1 TK due to the presence of Tyr172 [32], in VZV TK we can hypothesise that this interaction is much lower or absent because the residue Phe131 is not as polarisable as the corresponding tyrosine in HSV-1 TK. The hydrophobic interaction is probably weak due to an almost parallel alignment of the phenyl rings with the thymine ring. These hypotheses should be confirmed by further calculations.

The H-bonds formed with the two water molecules show some other important differences. As above stated, during the molecular dynamics simulations and minimisations the two crystal waters, also present in the HSV-1 TK binding site, were included without any restraints. As a result one of the two molecules, indicated as W2, moved relatively to its starting position, while the other water molecule W1 has the same relative position. The consequence is that the O4 of the thymine just forms one water-mediated H-bond instead of two as in HSV-1 TK (Fig. 2b). A molecular dynamic

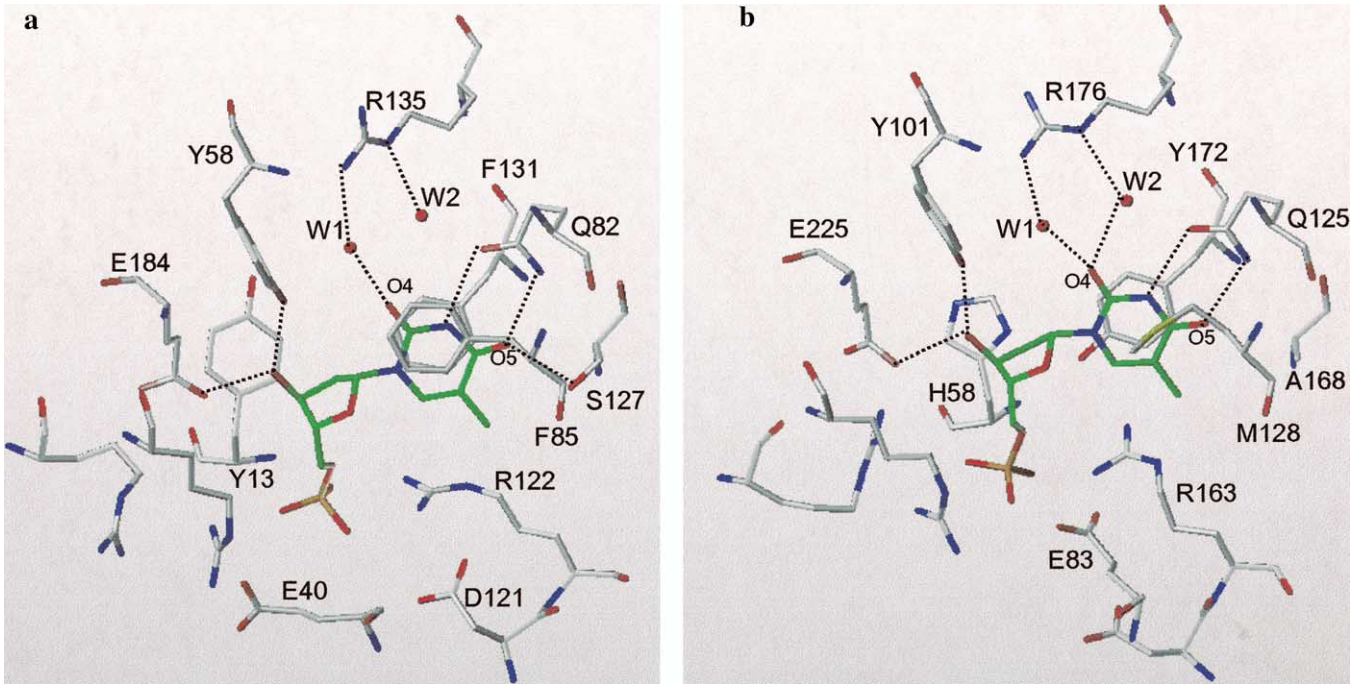

Fig. 2. Substrate-binding sites of VZV TK (a) and HSV-1 TK (b). Carbon atoms of TK and substrate (dTMP) are in white and green respectively, whereas the other atoms are color-coded (N, blue; O, red; S, yellow; P, orange). Dashed lines represent H-bonds. The criteria for defining the H-bonds were: the distance between hydrogen bond donor (D) and acceptor (A) is <3.2 Å and the angle between D–H···A is $>120°$.

simulation of HSV-1 TK under the same condition revealed that the water mediated H-bonds are stable (data not shown). The loss of this interaction however is compensated by an additional H-bond not present in HSV-1 TK, formed by Ser127 and O5 of the thymidine moiety. This interaction cannot be formed in HSV-1 TK because Ser127 is substituted with an alanine residue (Ala168). The net balance of H-bonds formed in HSV-1 TK and VZV TK is conserved and this is in agreement with the experimental fact that dT has the same affinity for VZV TK and HSV-1 TK [16,18].

In order to investigate the predictivity of our model as well as the characteristics of the binding with other substrates, we carried out docking studies. We docked first dT, which is the natural substrate, and dTMP in order to validate the docking protocol for VZV TK. The same protocol was previously used with HSV-1 TK and allowed the reproduction of the experimentally determined binding orientation of dT and ACV [30]. Fig. 3 shows the superimposition of the modelled dTMP (shown in green) with the docked dT (in magenta). As it is apparent the docking reproduces almost exactly the modelled orientation, with an rmsd of 0.6 Å. The same result was obtained with the docking of dTMP (data not shown).

After this validation the pyrimidine analogue brivudine (BVDU) and the guanosine analogues acyclovir (ACV) and ganciclovir (GCV) were docked.

As above mentioned, the water molecules present in the binding site of TK were removed only for the docking of the guanine analogues ACV and GCV, while they were taken into consideration when docking pyrimidine analogues (dT, dTMP and BVDU). This was based on the results of Pospisil et al. [30] who found that the AUTODOCK program failed to reproduce the crystallographic pose of guanine analogues when water was considered within the site, and the opposite was found for pyrimidine analogues. The lowest energy orientation has been considered for the evaluation of the binding mode of the ligands. Fig. 4a shows the docking result of BVDU. The ligand binds in a slightly different orientation in respect with dTMP (Fig. 2a), due to the presence of the bulkier brome vinyl group. This reorientation has only minor effects on the H-bonds pattern. Solely the distance between the 3′-OH group of BVDU and the OH-group of Tyr58 increases to 3.4 Å corresponding to a weaker H-bond. In comparison with the crystal structure of the complex HSV-1 TK/BVDU (Fig. 4b) [21], the presence of a weaker H-bond with the sugar moiety is in agreement with the slight decrease in binding affinity of BVDU towards VZV TK ($K_m = 0.78$ μM) compared to HSV-1 TK ($K_m = 0.50$ μM) [33].

Fig. 5a shows the docking result of ACV. The comparison with the corresponding crystal structure of HSV-1 TK [21] (Fig. 5b) shows that the molecule has a different orientation, especially concerning the base moiety. This is due to the presence of the residue Ser127, which forms two hydrogen bonds with N1 and N2 of ACV, and strongly affects the binding mode of the ligand. The consequences of this difference are that

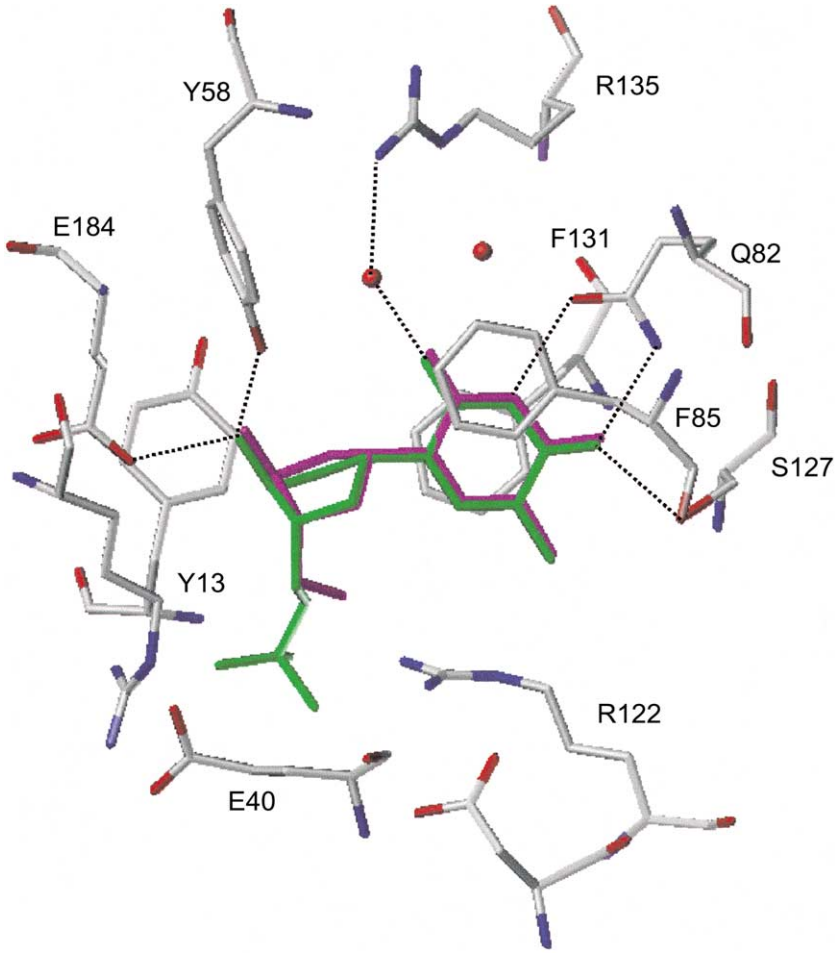

Fig. 3. Superimposition of docked dT (magenta) and the modelled dTMP (green) in the VZV TK binding site. The TK atoms are color-coded. Dashed lines represent H-bonds defined as mentioned in Fig. 2.

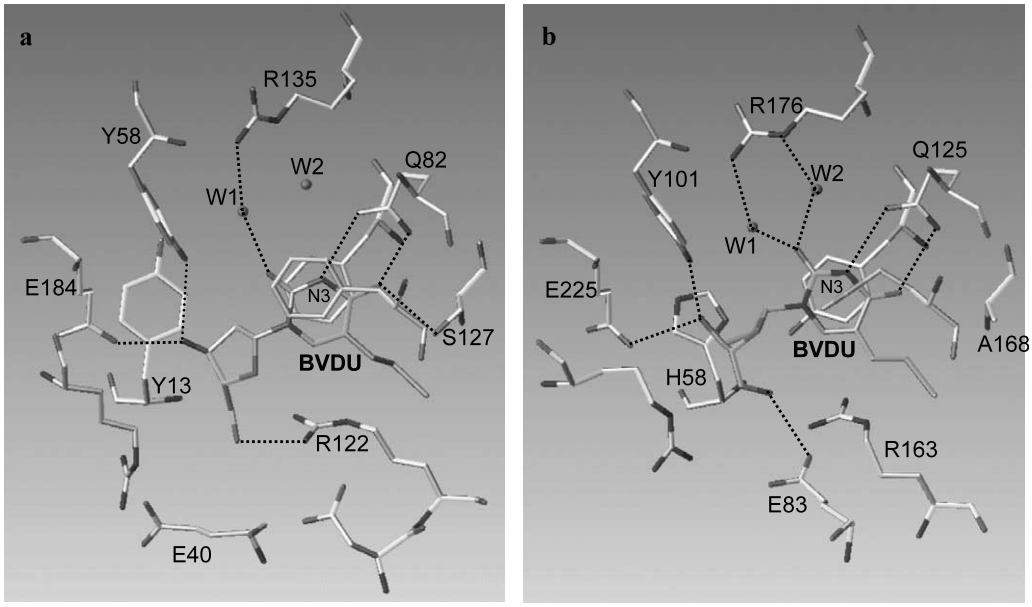

Fig. 4. Binding of BVDU (lowest energy orientation) in VZV TK (a) as resulting from docking studies, and in HSV-1 TK (b) crystal structure [21]. Dashed lines represent hydrogen bonds defined as mentioned in Fig. 2. Dotted line between 3′-OH group and the OH-group of Tyr58 represents the weak H-bond with a distance of 3.4 Å.

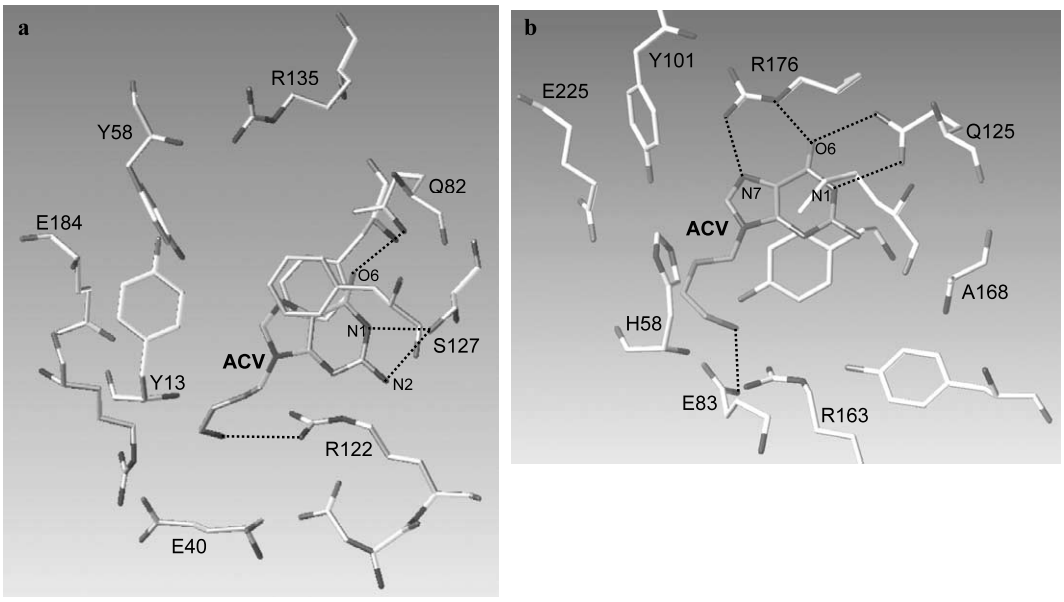

Fig. 5. Binding of ACV (lowest energy orientation) in VZV TK (a) as resulting from docking studies, and in HSV-1 TK (b) crystal structure [21]. Dashed lines represent hydrogen bonds defined as mentioned in Fig. 2.

the H-bonds with Arg135 (Arg176 in HSV-1 TK) are here missing, and also the sandwich-like interaction of the base moiety with Phe85 and Phe131 is not anymore present. Moreover, Gln82 forms a H-bond only with O6 of ACV; therefore the Watson–Crick interaction is missing meaning that the switching of the amide moiety of this amino acid is not necessary for the binding of ACV. The reduced H-bond pattern depicted by the docking is in agreement with the decrease of binding affinity of ACV towards VZV TK ($K_m > 500$ μM) [34] compared to HSV-1 TK ($K_m = 200$ μM) [16].

Interestingly, the GCV docking (Fig. 6a) does not show any significant differences in respect with the ACV binding (Fig. 5a) and compared with the corresponding crystal structure in HSV-1 TK [21] (Fig. 6b), in spite of the experimental evidence that GCV is not phosphorylated by VZV TK. However, this result is not isolated in the TK history, because already with HSV-1 TK it has been observed with X-ray studies that the inhibitor HBPG shares a common binding mode with the substrate ACV [19]. A rational explanation behind this experimental result has been given in a recent work

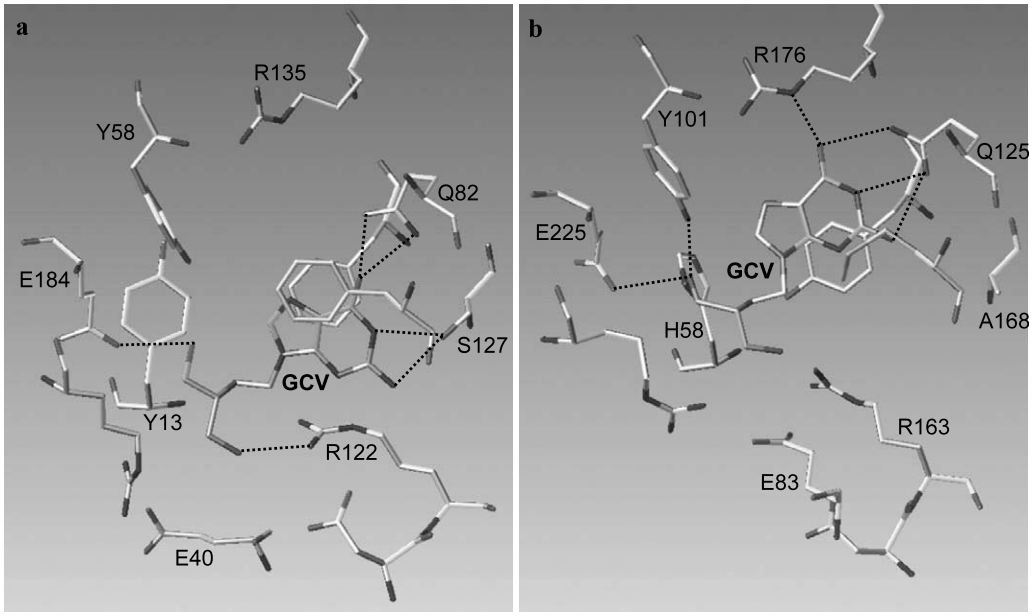

Fig. 6. Binding of GCV (lowest energy orientation) in VZV TK (a) as resulting from docking studies, and in HSV-1 TK (b) crystal structure [21]. Dashed lines represent hydrogen bonds defined as mentioned in Fig. 2.

combining biochemical data with ab initio calculations [35]. The authors could show that the catalytic activity is directly linked to the sugar-moiety dipole and its orientation within the binding site, and that the nucleo-base has an additive contribution. From this work the contribution to the catalytic constant (K_{cat}) of the GCV side chain is indeed lower compared to ACV. Considering the similarity of the HSV-1 TK and VZV TK binding sites it can be hypothesised that the different activity between ACV and GCV may be related to different K_{cat} contribution of the GCV side chain compared to ACV.

Further experimental, e.g., determination of catalytic activity for more compounds, and theoretical work has to be performed in order to assess this hypothesis.

4. Conclusions

In this work we described the homology modelling and docking studies on VZV TK: these studies resulted in a reliable model and allowed us to shed new light on the binding features of this enzyme, which has not yet been crystallised. In particular we found that there are slight differences in the way VZV TK binds the substrates in respect with HSV-1 TK (our template). These differences could be exploited for future ligand design in order to obtain more selective drugs for antiviral and gene therapy interventions.

References

[1] A. Arvin, in: P. Fields, D. Knipe, P. Howley (Eds.), Varicella Zoster Virus in Fields Virology, Raven, New York, 1995, pp. 2547–2586.
[2] J. Cohen, S. Straus, in: P. Fields, D. Knipe, P. Howley (Eds.), Varicella Zoster Virus and Its Replication in Fields Virology, Raven, New York, 1995, pp. 2525–2546.
[3] D.J. McGeoch, S. Cook, A. Dolan, F.E. Jamieson, E.A.R. Telford, J. Mol. Biol. 247 (1995) 443–458.
[4] B. Roizman, A.E. Sears, in: P. Fields, D. Knipe, P. Howley (Eds.), Herpes Simplex Viruses and Their Replication in Fields Virology, Raven, New York, 1995.
[5] P.R. Cohen, V.P. Beltrani, M.E. Grossman, Am. J. Med. 84 (1988) 1076–1080.
[6] S. Schimpff, A. Serpick, B. Stoler, B. Rumack, H. Mellin, J.M. Joseph, J. Block, Ann. Int. Med. 76 (1972) 241–254.
[7] C.E. Taylor, L. Sviland, A.D. Pearson, M. Dobb, M.W. Reid, J. Kernahan, A.W. Craft, P.J. Hamilton, S. Proctor, J. Clin. Pathol. 43 (1990) 633–637.
[8] K.W. Culver, Z. Ram, S. Wallbridge, H. Ishii, E.H. Oldfield, R.M. Blaese, Science 256 (1992) 1550–1552.
[9] C. Bonini, G. Ferrari, S. Verzeletti, P. Servida, E. Zappone, L. Ruggieri, M. Ponzoni, S. Rossini, F. Mavilio, C. Traversari, C. Bordignon, Science 276 (1997) 1719–1724.
[10] M.S. Chen, W.H. Prusoff, J. Biol. Chem. 253 (1978) 1325–1327.
[11] M.S. Chen, J. Walker, W.H. Prusoff, J. Biol. Chem. 254 (1979) 10747–10753.
[12] A.S. Waldman, E. Haeusslein, G. Milman, J. Biol. Chem. 258 (1983) 11571–11575.
[13] P.M. Keller, J.A. Fyfe, L. Beauchamp, C.M. Lubbers, P.A. Furman, H.J. Schaeffer, G.B. Elion, Biochem. Pharmacol. 30 (1981) 3071–3077.
[14] B.A. Larder, Y.C. Cheng, G. Darby, J. Gen. Virol. 64 (1983) 523–532.
[15] D.F. Smee, J.C. Martin, J.P. Verheyden, T.R. Matthews, Antimicrob. Agents Chemother. 23 (1983) 676–682.
[16] B.D. Pilger, R. Perozzo, F. Alber, C. Wurth, G. Folkers, L. Scapozza, J. Biol. Chem. 274 (1999) 31967–31973.
[17] A. Prota, J. Vogt, R. Perozzo, B.D. Pilger, C. Wurth, V. Marquez, P. Russ, G. Schulz, G. Folkers, L. Scapozza, Biochemistry 39 (2000) 9597–9603.
[18] I. Amrhein, C. Wurth, T. Bohner, R. Hofbauer, G. Folkers, L. Scapozza, Protein Expres. Purif. 18 (2000) 338–345.
[19] M.S. Bennett, F. Wien, J.N. Champness, T. Batuwangala, T. Rutherford, W.C. Summers, H. Sun, G. Wright, M.R. Sanderson, FEBS Lett. 443 (1999) 121–125.
[20] D.G. Brown, R. Visse, G. Sandhu, A. Davies, P.J. Rizkallah, C. Melitz, W.C. Summers, M.R. Sanderson, Nat. Struct. Biol. 2 (1995) 876–881.
[21] J.N. Champness, M.S. Bennett, F. Wien, R. Visse, W.C. Summers, P. Herdewijn, E. de Clerq, T. Ostrowski, R.L. Jarvest, M.R. Sanderson, Proteins 32 (1998) 350–361.
[22] K. Wild, T. Bohner, A. Aubry, G. Folkers, G.E. Schulz, FEBS Lett. 368 (1995) 289–292.
[23] K. Wild, T. Bohner, G. Folkers, G.E. Schulz, Protein Sci. 6 (1997) 2097–2106.
[24] W.R. Person, T. Wood, Z. Zhang, W. Miller, Genomics 46 (1997) 24–36.
[25] SYBYL, TRIPOS Inc., St. Louis, Missouri.
[26] R.A. Laskowski, M.W. McArthur, D.S. Moos, J.M.J. Thornton, Appl. Cryst. 26 (1993) 283–291.
[27] AMBER 5, University of California, San Francisco.
[28] J.-P. Ryckaert, G. Ciccotti, H.G.C. Berendsen, J. Comput. Phys. 23 (1977) 327–341.
[29] G.M. Morris, D.S. Goodsell, R.S. Halliday, R. Huey, W.E. Hart, R.K. Belew, A.J. Olson, J. Comput. Chem. 19 (1998) 1639–1662.
[30] P. Pospisil, L. Scapozza, G. Folkers, Proceedings of the 13th European Symposium on QSAR-Rational Approaches in Drug Design, 2001, pp. 92–96.
[31] J. Gasteiger, M. Marsili, Tetrahedron 36 (1980) 3219–3228.
[32] F. Alber, O. Kuonen, L. Scapozza, G. Folkers, P. Carloni, Proteins: Struct. Funct. Genet. 31 (1998) 453–459.
[33] R. Sienaert, L. Naesens, A. Brancale, E. de Clerq, C. McGuigan, J. Balzarini, Mol. Pharmacol. 61 (2002) 249–254.
[34] T. Suzutani, L.C. Davies, R.W. Honess, J Gen. Virol. 74 (1993) 1011–1016.
[35] M. Sulpizi, P. Schelling, G. Folkers, P. Carloni, L. Scapozza, J. Biol. Chem. 276 (2001) 21692–21697.